Int. J. Heat Mass Transfer. Vol. 27, No. 12, pp. 2215–2224, 1984
Printed in Great Britain

0017-9310/84 $3.00 + 0.00

A formulation of combined forced and free convection past horizontal and vertical surfaces

M. S. RAJU, X. Q. LIU and C. K. LAW
Department of Mechanical and Nuclear Engineering, Northwestern University, Evanston, IL 60201, U.S.A.

(*Received* 13 *May* 1983 *and in revised form* 2 *December* 1983)

Abstract—The boundary-layer flow over semi-infinite vertical and horizontal flat plates, heated to a constant temperature in a uniform free stream, is studied when the buoyancy forces either aid or oppose the development of the boundary layer. Different mixed-convection parameters are introduced in the formulation of the respective problems involving horizontal and vertical surfaces such that smooth transition from one convective limit to the other is possible; in particular the governing equations for the purely forced and free convection cases are respectively recovered from the zero values of the Grashoff and Reynolds numbers. An effective numerical scheme is developed to incorporate the integral boundary condition appearing in the governing equations of the flow over a horizontal flat plate, thereby rendering numerical convergence possible. Locally similar and locally nonsimilar solutions are also obtained. They show considerable deviation of the velocity profiles from the rigorous finite-difference solution in the region of intense mixed convection, although good agreement exists for the wall values, as represented by the friction factors and Nusselt numbers, which are of primary interest. Simple explicit expressions correlating local Nusselt numbers over the entire range of mixed convection intensity when Prandtl numbers vary from 0.1 to 10 are determined. The separation points in opposing flows are also obtained.

1. INTRODUCTION

BUOYANT forces play an important role in the force convective flow over solid bodies by altering the flow field and hence the heat transfer and shear stress characteristics at the wall. Extensive studies [1–11] have been conducted on mixed-convective flow over horizontal or vertical flat surfaces. In these studies the formulation fails to provide a smooth transition between the forced convective limit and the free convective limit in that, depending on whether the Grashoff number (Gr) or Reynolds number (Re) is used for nondimensionalization, the solution becomes increasingly difficult to obtain as one of these limits is approached. In fact the solution becomes singular at the respective limit.

Recently, during the study of the diffusion flame structure in stagnation flows, Fernandez-Pello and Law [12] introduced a unified mixed-flow parameter of the form $(Re^4 + Gr^2)^{1/8}$ for nondimensionalization. The resulting formulation provides solutions which are uniformly valid over the entire range of the mixed-convective flow between the two limits. Furthermore, since the formulation removes the singularity appearing at one of the limits, the governing equations then become similar at both limits. This formulation subsequently has also been applied to the diffusive burning over vertical surfaces [13].

In the present study we have extended the formulation and solution of the mixed-flow problem in several aspects.

(1) Analogous to the mixed-flow parameter for vertical plates, we have introduced a corresponding parameter of the form $(Re^5 + Gr^2)^{1/10}$ for the horizontal surface.

(2) We have also found it useful to introduce new transformed x-coordinates, ξ, of the forms $(1 + Gr^2/Re^4)^{-1}$ and $(1 + Gr^2/Re^5)^{-1}$, instead of the conventional forms of Gr/Re^2 and $Gr/Re^{5/2}$, for the vertical and horizontal surfaces, respectively. Use of these new coordinates properly places the flow range to be between $\xi = (0, 1)$, and thereby facilitates the solution procedure.

(3) We have developed a numerical scheme in which convergence in the horizontal case is achieved [1].

(4) Solutions for both aiding and opposing flows have been obtained; in the latter case the separation points have also been determined.

(5) Both local-similarity and local non-similarity solutions have been obtained and compared with the rigorous solutions.

We now present the formulation and solutions mentioned above.

2. VERTICAL FLAT PLATE

The conservation equations when the buoyancy forces influence the development of the boundary layer flow over a vertical flat surface are given by

$$\frac{\partial(\rho u)}{\partial x} + \frac{\partial(\rho v)}{\partial y} = 0 \tag{1}$$

$$\rho u \frac{\partial u}{\partial x} + \rho v \frac{\partial u}{\partial y} = \frac{\partial}{\partial y}\left(\mu \frac{\partial u}{\partial y}\right) \pm \rho g \beta (T - T_\infty) \tag{2}$$

$$\rho u \frac{\partial T}{\partial x} + \rho v \frac{\partial T}{\partial y} = \frac{\partial}{\partial y} \rho \left(\frac{\lambda}{c_p} \frac{\partial T}{\partial y}\right). \tag{3}$$

The second term on the RHS of equation (2) is due to the buoyancy induced force. The boundary conditions for

NOMENCLATURE

c_p specific heat
C_f local skin friction factor
F reduced stream function
g gravitational acceleration
Gr local Grashoff number, $g\beta(T_w - T_\infty)x^3/\nu^2$
Nu Nusselt number
Pr Prandtl number
Re local Reynolds number, $U_\infty x/\nu$
T fluid temperature
T_w wall temperature
T_∞ free stream temperature
u axial velocity component
U_∞ free stream velocity
v normal velocity component
x axial coordinate
y transverse coordinate.

Greek symbols
α thermal diffusivity
β coefficient of thermal expansion
η pseudo-similarity variable
θ dimensionless temperature, $(T - T_\infty)/(T_w - T_\infty)$
λ thermal conductivity
μ dynamic viscosity
ν kinematic viscosity
ξ present mixed-convection parameter: $(1 + Gr^2/Re^4)^{-1}$ for vertical case; $(1 + Gr^2/Re^5)^{-1}$ for horizontal case
ξ_1 conventional mixed-convection parameter for vertical case, Gr/Re^2
ξ_2 conventional mixed-convection parameter for horizontal case, $Gr/Re^{5/2}$
ξ_s separation point
ρ density
ψ stream function.

Superscript
denotes partial derivative with respect to η.

equations (1)–(3) are

$$u = v = 0, \quad T = T_w \quad \text{at} \quad y = 0$$
$$u \to U_\infty, \quad T \to T_\infty \quad \text{as} \quad y \to \infty \tag{4}$$
$$u = U_\infty, \quad T = T_\infty \quad \text{at} \quad x = 0.$$

To facilitate the solution of the above system of equations over the entire regime of mixed, forced, and free convection, it is necessary to transform these equations to a form which exhibits the effects of buoyancy on forced convection and also the effects of forced flow on free convection. The mathematical analysis is simplified by introducing the following coordinates of transformation

$$\xi = \xi(x), \quad \eta = \frac{Re^{1/2}}{x\xi^{1/8}} \int_0^y (\rho/\rho_\infty)\, dy. \tag{5}$$

In addition, a reduced stream function $F(\xi, \eta)$ and a dimensionless temperature $\theta(\xi, \eta)$ are defined, respectively, as

$$\psi(\xi, \eta) = \frac{Re^{1/2}}{\xi^{1/8}} F(\xi, \eta), \quad \theta(\xi, \eta) = \frac{T - T_\infty}{T_w - T_\infty} \tag{6}$$

where $\psi(\xi, \eta)$ is the stream function that satisfies the continuity equation (1) and

$$\rho u = \mu_\infty \frac{\partial \psi}{\partial y}, \quad \rho v = -\mu_\infty \frac{\partial \psi}{\partial x}. \tag{7}$$

Assuming constant values for $\rho\mu$, c_p, and $\rho\lambda$, the transformed system of equations become

$$F''' + \frac{(3-\xi)}{4} FF'' - \frac{(1-\xi)}{2} F'^2 \pm \sqrt{(1-\xi)}\theta = 2(1-\xi)\xi\left[F'' \frac{\partial F}{\partial \xi} - F' \frac{\partial F'}{\partial \xi}\right] \tag{8}$$

$$\theta'' + \frac{Pr(3-\xi)}{4} F\theta' = 2Pr\,\xi(1-\xi)\left[\theta' \frac{\partial F}{\partial \xi} - F' \frac{\partial \theta}{\partial \xi}\right] \tag{9}$$

$$F'(\xi, 0) = 0, \quad \theta(\xi, 0) = 1 \tag{10a}$$

$$(3-\xi)F(\xi, 0) - 8\xi(1-\xi)\frac{\partial F(\xi, 0)}{\partial \xi} = 0 \tag{10b}$$

$$F'(\xi, \infty) = \xi^{1/4}, \quad \theta(\xi, \infty) = 0. \tag{10c}$$

In the above equations, primes denotes partial differentiation with respect to η, Pr is the Prandtl number, and $\xi(x)$, which serves as the buoyancy parameter in the forced convection limit and as the forced convection parameter in the free convection limit, is given by

$$\xi = \left(1 + \frac{Gr^2}{Re^4}\right)^{-1} \tag{11}$$

where $Gr = g\beta(T_w - T_\infty)x^3/\nu^2$, $Re = U_\infty x/\nu$ are the local Grashoff and Reynolds numbers, respectively.

It is seen from the present formulation of the problem that the governing equations reduce to forced and free convection limits, respectively, when $\xi = 1$ and 0. Both the limits have similarity solutions. Equations (8)–(10) are solved using a finite-difference scheme similar to that given in the Appendix. The same equations are also solved by utilizing the local similarity and local non-similarity methods. In the local similarity method the governing equations reduce to ordinary differential equations by eliminating the terms involving the derivations with respect to ξ. In the local non-similarity method of Sparrow and Yu [14], the solutions are truncated at the second level by eliminating the terms involving the second order derivatives with respect to ξ.

3. HORIZONTAL FLAT PLATE

The conservation equations for the laminar boundary layer flow with mixed convection over a horizontal flat plate are given by

$$\frac{\partial(\rho u)}{\partial x}+\frac{\partial(\rho v)}{\partial y}=0 \tag{12}$$

$$\rho u\frac{\partial u}{\partial x}+\rho v\frac{\partial u}{\partial y}=\frac{\partial}{\partial y}\left(\mu\frac{\partial u}{\partial y}\right)\pm g\beta\frac{\partial}{\partial x}\left[\int_y^\infty \rho(T-T_\infty)\,dy\right] \tag{13}$$

$$\rho u\frac{\partial T}{\partial x}+\rho v\frac{\partial T}{\partial y}=\frac{\partial}{\partial y}\left(\frac{\lambda}{c_p}\frac{\partial T}{\partial y}\right). \tag{14}$$

The second term on the RHS of equation (13), derived in detail by Sparrow and Minkowycz [3], is the streamwise pressure gradient due to buoyancy. The boundary conditions for equations (13) and (14) are

$$\begin{aligned} &u=v=0, \quad T=T_w \quad \text{at} \quad y=0\\ &u\to U_\infty, \quad T\to T_\infty \quad \text{as} \quad y\to\infty\\ &u=U_\infty, \quad T=T_\infty \quad \text{at} \quad x=0. \end{aligned} \tag{15}$$

It may also be noted that the problem can also be formulated, in a somewhat more straightforward fashion, without the integral representation in equation (13). We have, however, purposefully adopted the integral formulation in order to demonstrate the features of the present numerical scheme which removes the convergence difficulty reported in ref. [1], and is expected to have extended utility in other situations.

To facilitate the solution of the above equations for the entire range of mixed convection, the following set of coordinates are introduced

$$\eta=\frac{Re^{1/2}}{x\xi^{1/10}}\int_0^y(\rho/\rho_\infty)\,dy, \quad \xi=\left(1+\frac{Gr^2}{Re^5}\right)^{-1}. \tag{16}$$

In addition, a reduced stream function and a dimensionless temperature $\theta(\xi,\eta)$ are defined as

$$\psi(\xi,\eta)=\frac{Re^{1/2}}{\xi^{1/10}}F(\xi,\eta), \quad \theta(\xi,\eta)=\frac{T-T_\infty}{T_w-T_\infty} \tag{17}$$

where ψ is the stream function which satisfies equation (12). Making use of the Boussinesq approximation, the transformed system of equations become

$$F''''+\frac{(6-\xi)}{10}FF'''+\frac{(2+3\xi)}{10}F'F''\pm\sqrt{(1-\xi)}\frac{(4+\xi)}{10}\eta\theta'=\xi(1-\xi)\left[F'''\frac{\partial F}{\partial\xi}-F'\frac{\partial F''}{\partial\xi}\mp\sqrt{(1-\xi)}\frac{\partial\theta}{\partial\xi}\right] \tag{18}$$

$$\theta''+\frac{Pr(6-\xi)}{10}F\theta'=Pr\,\xi(1-\xi)\left[\theta'\frac{\partial F}{\partial\xi}-F'\frac{\partial\theta}{\partial\xi}\right] \tag{19}$$

$$F'(\xi,0)=0, \quad (6-\xi)F(\xi,0)-10\xi(1-\xi)\frac{\partial F(\xi,0)}{\partial\xi}=0, \quad \theta(\xi,0)=1 \tag{20a}$$

$$F'''(\xi,0)=\sqrt{(1-\xi)}\left\{\mp\frac{(4+\xi)}{10}\int_0^\infty\theta\,d\eta\pm\xi(1-\xi)\int_0^\infty\frac{\partial\theta}{\partial\xi}\,d\eta\right\} \tag{20b}$$

$$F'(\xi,\infty)=\xi^{1/5}, \quad \theta(\xi,\infty)=0 \tag{20c}$$

where primes denotes partial differentiation with respect to η. As in the previous formulation, the governing equations reduce to forced and free convection limits, respectively, when $\xi=1$ and 0. Both limits have similarity solutions. Equations (18)–(20) are solved using an identical finite-difference scheme that is given in the Appendix and also by the local similarity method.

4. RESULTS AND DISCUSSIONS

Numerical calculations are carried out for fluids having Prandtl numbers of 0.1, 0.7, 1.0, and 10.0 over the entire regime of mixed, forced and free convective flow over vertical and horizontal flat surfaces. A finite-difference scheme has been developed and is detailed in the Appendix. The scheme is based on the method of quasi-linearization and iteration to integrate the respective governing equations in the entire range of mixed convection parameter $0.0<\xi<1.0$. In order to verify the accuracy of using the local similarity approximation under the present formulation, the equations under this approximation are also solved using the quasi-linearization scheme. Additionally, the local non-similarity method of Sparrow and Yu [14] has also been used for comparison purpose in the case involving the vertical surface. Local non-similarity solutions for the horizontal case have not been obtained because of the excessive computing cost and because they are not expected to provide any new insight in addition to those of the vertical case.

The primary physical quantities of interest are the velocity distribution $(u/U_\infty)=F'(\xi,\eta)$, the temperature distribution $(T-T_\infty)/(T_w-T_\infty)=\theta(\xi,\eta)$, the local Nusselt number Nu, and the local skin friction factor C_f. The last two quantities are defined, respectively, by

$$Nu=\frac{Q_w}{(T_w-T_\infty)}\frac{x}{\lambda}, \quad C_f=\frac{\tau_w}{\rho U_\infty^2/2} \tag{21}$$

where $\tau_w=\mu(\partial u/\partial y)_{y=0}$ is the wall shear stress and $Q_w=-\lambda(\partial T/\partial y)_{y=0}$ is the wall heat flux. Making use of equations (5)–(7), we get

$$Nu/\sqrt{Re}=-\frac{\theta'(\xi,0)}{\xi^{1/8}}, \quad C_f\sqrt{Re}=\frac{2F''(\xi,0)}{\xi^{3/8}} \tag{22}$$

which are applicable for the case of the vertical flat plate. Similarly, for the case of the horizontal flat plate and using equation (16) and (17) we get

$$Nu/\sqrt{Re}=-\frac{\theta'(\xi,0)}{\xi^{1/10}}, \quad C_f\sqrt{Re}=\frac{2F''(\xi,0)}{\xi^{3/10}}. \tag{23}$$

Table 1 and Figs. 1–4 correspond to the case of the vertical flat surface when buoyancy force aids the

Table 1. Results of $F''(\xi,0)$ and $-\theta'(\xi,0)$ for mixed-convective flow over vertical surfaces

		$Pr = 0.1$		Rigorous solution $Pr = 0.7$		$Pr = 1.0$		$Pr = 10.0$		Local non-similarity method $Pr = 0.7$		Local similarity method $Pr = 0.7$	
ξ	ξ_1	$F''(\xi,0)$	$-\theta'(\xi,0)$	$F''(\xi,0)$	$-\theta'(\xi,0)$	$F''(\xi,0)$	$-\theta'(\xi,0)$	$F''(\xi,0)$	$-\theta'(\xi,0)$	$F''(\xi,0)$	$-\theta'(\xi,0)$	$F''(\xi,0)$	$-\theta'(\xi,0)$
1.00000	0.000	0.3321	0.1520	0.3321	0.2928	0.3321	0.3275	0.3321	0.7290	0.3321	0.2928	0.3321	0.2928
0.92237	0.290	0.6452	0.1716	0.5919	0.3373	0.5795	0.3825	0.4886	0.8137	0.6562	0.3419	0.6310	0.3297
0.84935	0.421	0.7683	0.1772	0.6889	0.3505	0.6706	0.3972	0.5413	0.8366	0.7666	0.3529	0.7055	0.3368
0.78075	0.530	0.8514	0.1804	0.7536	0.3584	0.7310	0.4061	0.5758	0.8507	0.8327	0.3584	0.7520	0.3414
0.71639	0.629	0.9145	0.1825	0.8020	0.3639	0.7763	0.4122	0.6010	0.8604	0.8736	0.3613	0.7859	0.3448
0.65610	0.724	0.9651	0.1839	0.8404	0.3680	0.8121	0.4167	0.6205	0.8676	0.8993	0.3628	0.8125	0.3478
0.40960	1.201	1.1526	0.1887	0.9743	0.3823	0.9346	0.4324	0.6772	0.8861	0.9462	0.3654	0.8930	0.3582
0.24010	1.779	1.2202	0.1869	1.0171	0.3828	0.9728	0.4330	0.6897	0.8864	0.9631	0.3685	0.9329	0.3642
0.12960	2.592	1.2437	0.1840	1.0282	0.3794	0.9819	0.4296	0.6860	0.8810	0.9722	0.3709	0.9540	0.3671
0.06250	3.873	1.2468	0.1815	1.0251	0.3751	0.9776	0.4251	0.6738	0.8728	0.9758	0.3715	0.9642	0.3676
0.02560	6.169	1.2397	0.1796	1.0145	0.3706	0.9661	0.4202	0.6571	0.8630	0.9754	0.3701	0.9678	0.3665
0.00810	11.066	1.2273	0.1782	1.0002	0.3662	0.9510	0.4153	0.6387	0.8527	0.9723	0.3673	0.9673	0.3642
0.00160	24.980	1.2128	0.1769	0.9848	0.3619	0.9345	0.4105	0.6203	0.8428	0.9677	0.3632	0.9645	0.3611
0.00010	99.995	1.1979	0.1754	0.9699	0.3576	0.9182	0.4057	0.6032	0.8334	0.9624	0.3584	0.9609	0.3573
0.00000	∞	1.1839	0.1739	0.9570	0.3531	0.9034	0.4006	0.5881	0.8240	0.9570	0.3531	0.9570	0.3531

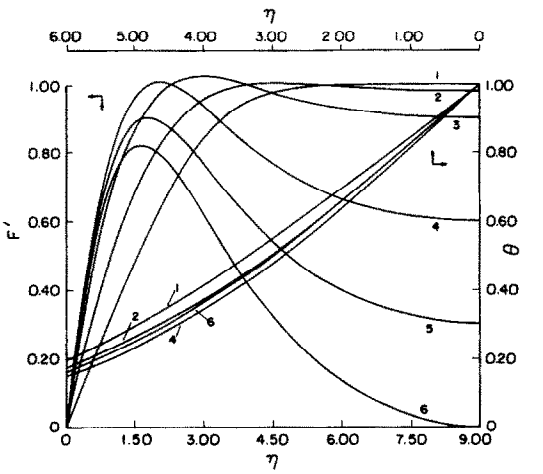

FIG. 1. Velocity and temperature profiles for $Pr = 0.1$ for mixed convective flow over vertical surfaces. Curves 1–6 designate $\xi = 1.0$, 0.9224, 0.6561, 0.1296, 0.0081, and 0, respectively.

development of the boundary layer. The local Nusselt number and the local skin friction factors can be evaluated from the values of ξ, $F''(\xi,0)$, $\theta'(\xi,0)$ using equation (22). The results confirm the observations of previous works [1–11] that for all values of the buoyancy parameter, $\xi_1 = Gr/Re^2$, the local Nusselt number for the mixed, forced and free convection flows are higher than what would be in either of the pure buoyant and pure forced flows. In the case of mixed convective flow over a vertical flat surface, the buoyancy forces directly influence the fluid motion. Any increase in the buoyancy forces results in an enhanced fluid acceleration and thus also increases the Nusselt number. Significant deviations from the forced convection flow become apparent at low values of the buoyancy parameters, ξ_1. It can be seen from Figs. 1–4 and Table 1 that higher values of the thermal gradients are associated with fluids having larger Prandtl

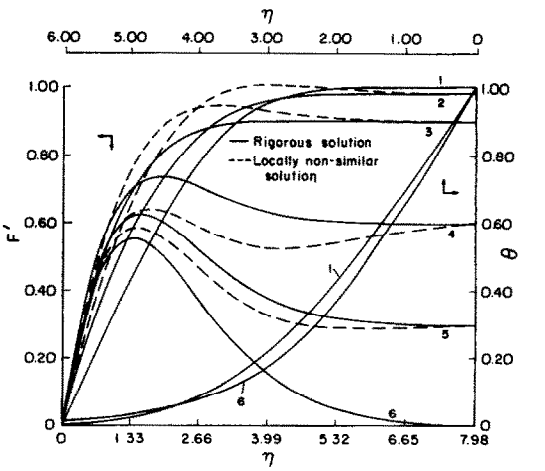

FIG. 2. Same as Fig. 1 except $Pr = 0.7$. Also shown are local non-similarity solutions.

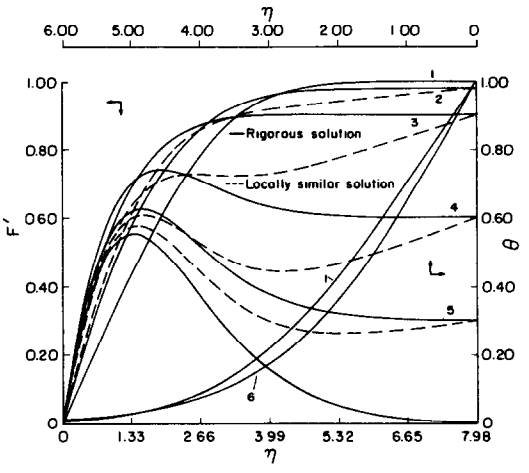

FIG. 3. Same as Fig. 1 except $Pr = 0.7$. Also shown are local similarity solutions.

numbers, because of the smaller boundary-layer thickness and hence a larger temperature gradient at the wall.

Figures 1–4 also show that the velocity overshoot above the free stream velocity can be quite large for low Prandtl numbers. Fluids with large Prandtl numbers are more sensitive to the effect of forced convection in the free convection limit. The location of the maximum velocity moves inward with an increase in the buoyancy effect, but the thickness of the thermal and velocity boundary layers remain constant for a given Prandtl number. As can be seen from Table 1, a higher value of $F''(\xi, 0)$ is associated with fluids having lower Prandtl numbers and $F''(\xi, 0)$ increases with an increase in the buoyancy parameter, ξ_1.

Figure 2 compares the velocity profiles of the rigorous solution with those obtained with the local non-similarity approximation, for $Pr = 0.7$. The temperature profiles are not compared because they are always quite close to each other. Table 1 demonstrates this close agreement for the wall values $\theta'(\xi, 0)$, which

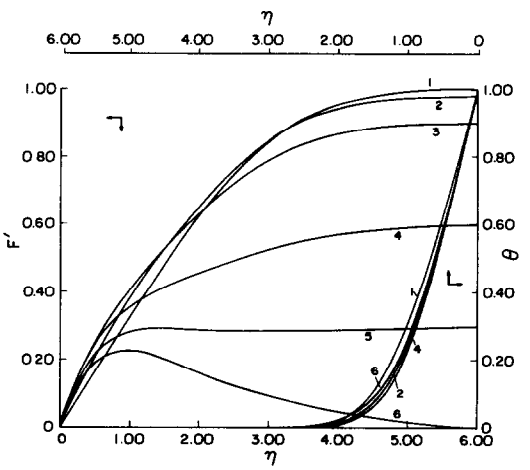

FIG. 4. Same as Fig. 1 except $Pr = 10.0$.

show a maximum difference of 4.4%. The velocity profiles, however, show substantial disagreement away from the wall in the region of intense mixed convection with $0.02 < \xi_1 < 3.5$. The maximum deviation in the wall values $F''(\xi, 0)$ is about 11%. These results are consistent with the greater sensitivity of the velocity profiles to the buoyancy induced forces, thereby making it more sensitive to approximations in the analysis.

Figure 3 and Table 1 compare the local similarity approximation to the rigorous solutions for $Pr = 0.7$. Here again we observe good agreement for the temperature results and substantial disagreement in the velocity profiles away from the wall in the region of the intense mixed convection. Maximum differences of 8.3 and 6.3% are observed for the wall values $F''(\xi, 0)$ and $\theta'(\xi, 0)$, respectively. The good agreement for $F''(\xi, 0)$ and $\theta'(\xi, 0)$ obtained by the rigorous and local similarity assumptions, in addition to the considerable simplifications the local similarity method introduces, suggest the use of this approximation for most practical purposes. It should also be noted that the conventional formulation of using only Reynolds or Grashoff numbers for non-dimensionalization of governing equations does not result in a local similarity solution as the other convection limit is approached; the governing equations in fact become singular at that limit.

We also note that in Figs. 2 and 3, and also Fig. 6 to be discussed later, the locally similar and the locally nonsimilar velocity profiles exhibit the existence of a local minima, at large values of η, whose value is even less than the free stream value. It has been ascertained that this is a consequence of the use of a finite free stream boundary in the numerical calculations, and that it has practically no effect on the wall values represented by the skin friction coefficient and the Nusselt number. Accuracy of the present numerical scheme has also been checked by using Gear's initial boundary value routine with the missing boundary condition $f''(\xi, 0)$ obtained from the present numerical solution. Numerical results from both schemes were identical.

Table 2 and Figs. 5–7 correspond to the case of the horizontal flat plate. The results show similar trends as those of the vertical case. The velocity overshoot is quite large for fluids having small Prandtl numbers when compared to the previous case and consequently result in higher values of $F''(\xi, 0)$ and $\theta'(\xi, 0)$ at the wall. However, at higher values of Prandtl numbers and larger values of the mixed convection parameter, ξ_2, the effect of forced convection flow in the free convection limit is less significant when compared to the vertical case. This results in lower values of $F''(\xi, 0)$ and $\theta'(\xi, 0)$ in this range of mixed convection flow. For $Pr = 0.7$, the maximum differences in $F''(\xi, 0)$ and $\theta'(\xi, 0)$ are 16 and 4.6%, respectively.

Under the current formulation it is observed from Tables 1 and 2 that there is only a slight variation of the dimensionless temperature gradient, $-\theta'(\xi, 0)$, with the mixed convection number for any given Prandtl

Table 2. Results of $F''(\xi,0)$ and $-\theta'(\xi,0)$ for mixed-convective flow over horizontal surfaces

		Rigorous solution								Local similarity method	
		$Pr = 0.1$		$Pr = 0.7$		$Pr = 1.0$		$Pr = 10.0$		$Pr = 0.7$	
ξ	ξ_2	$F''(\xi,0)$	$-\theta'(\xi,0)$	$F''(\xi,0)$	$-\theta'(\xi,0)$	$F''(\xi,0)$	$-\theta'(\xi,0)$	$F''(\xi,0)$	$-\theta'(\xi,0)$	$F''(\xi,0)$	$-\theta'(\xi,0)$
1.00000	0.000	0.3332	0.1527	0.3332	0.2931	0.3332	0.3328	0.3332	0.7289	0.3332	0.2931
0.90392	0.326	0.9472	0.1785	0.6306	0.3441	0.5904	0.3855	0.4196	0.7774	0.7334	0.3476
0.81537	0.476	1.1879	0.1887	0.7372	0.3582	0.6810	0.3999	0.4453	0.7884	0.8226	0.3571
0.73390	0.602	1.3450	0.1943	0.8042	0.3660	0.7375	0.4078	0.4600	0.7939	0.8726	0.3621
0.65908	0.719	1.4610	0.1979	0.8524	0.3711	0.7779	0.4129	0.4694	0.7969	0.9047	0.3653
0.59049	0.833	1.5518	0.2004	0.8893	0.3746	0.8085	0.4165	0.4756	0.7983	0.9268	0.3673
0.32768	1.432	1.9513	0.2125	1.0368	0.3896	0.9279	0.4307	0.4901	0.7969	0.9733	0.3713
0.16807	2.225	2.0596	0.2106	1.0629	0.3864	0.9447	0.4269	0.4754	0.7824	0.9835	0.3711
0.07776	3.444	2.0576	0.2060	1.0524	0.3798	0.9323	0.4197	0.4554	0.7665	0.9850	0.3696
0.03125	5.568	2.0268	0.2027	1.0342	0.3739	0.9143	0.4132	0.4352	0.7506	0.9843	0.3673
0.01024	9.831	2.0032	0.2009	1.0185	0.3695	0.8980	0.4079	0.4163	0.7349	0.9834	0.3647
0.00243	20.261	1.9946	0.1997	1.0071	0.3657	0.8848	0.4032	0.3992	0.7196	0.9830	0.3619
0.00032	55.893	1.9952	0.1983	0.9989	0.3618	0.8738	0.3983	0.3845	0.7049	0.9833	0.3591
0.00001	316.226	1.9984	0.1966	0.9924	0.3578	0.8643	0.3932	0.3723	0.6911	0.9846	0.3563
0.00000	∞	2.0005	0.1947	0.9869	0.3536	0.8556	0.3881	0.3624	0.6780	0.9869	0.3536

number. Advantage can be taken of this fact to correlate the local Nusselt number in terms of the Prandtl number, Pr, and mixed convection number, ξ. The following relationships apply, respectively, for the mixed convective flow over vertical and horizontal flat surfaces

$$\frac{Nu}{\sqrt{Re}} = -\frac{0.37Pr^{1/3}}{\xi^{1/8}} \tag{24}$$

$$\frac{Nu}{\sqrt{Re}} = -\frac{0.37Pr^{1/3}}{\xi^{1/10}}. \tag{25}$$

The local Nusselt numbers obtained from equations (24) and (25) are found to correlate within 20% accuracy the numerical data obtained for the *general and extensive* parametric range of any given mixed convection number and Prandtl number, with $0.1 < Pr < 10$.

For opposing flows the buoyancy force acts like an

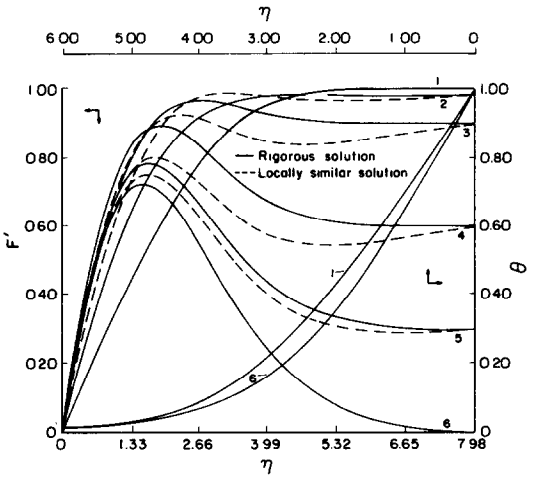

FIG. 6. Same as Fig. 5 except $Pr = 0.7$. Also shown are local similarity solutions.

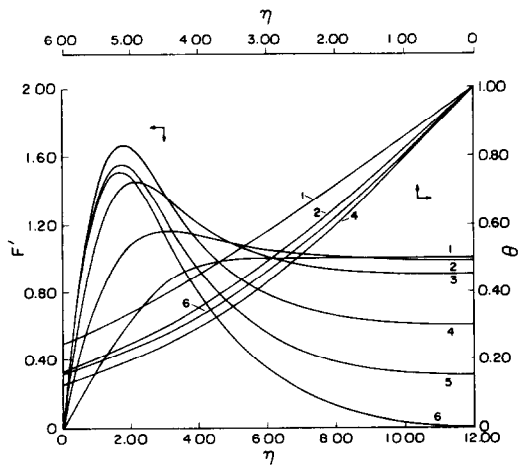

FIG. 5. Velocity and temperature profiles for $Pr = 0.1$ for mixed convective flow over horizontal surfaces. Curves 1–6 designate $\xi = 1.0$, 0.9039, 0.5904, 0.07776, 0.00293, and 0, respectively.

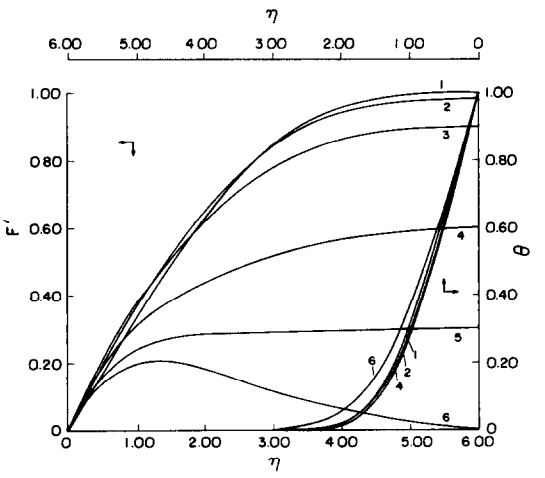

FIG. 7. Same as Fig. 5 except $Pr = 10.0$.

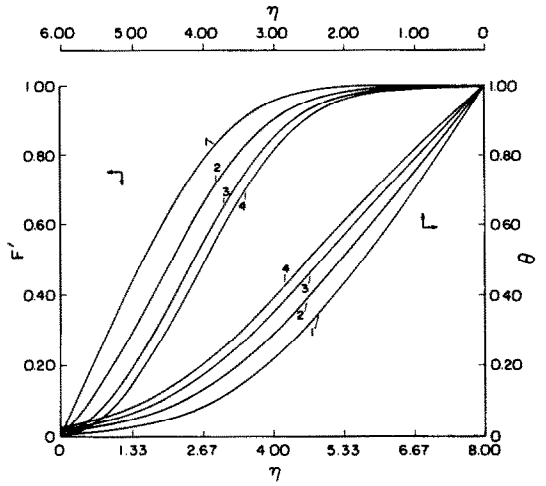

FIG. 8. Temperature and velocity profiles for opposing mixed convective flow over vertical surfaces, for $Pr = 0.7$. Curves 1–4 designate $\xi_1 = 0.0$, 0.1271, 0.1807, and 0.1865, respectively.

adverse pressure gradient which tends to cause separation of the boundary layer. Figures 8 and 9 show the representative velocity and temperature profiles for the two cases of horizontal and vertical plates when buoyancy force opposes the development of the boundary layer, with $Pr = 0.7$. The opposing buoyancy force reduces the velocity and velocity gradients at the wall as compared to those in pure forced convection. The thermal gradient at the wall decreases and the thermal boundary layer thickness increases as the separation point is approached. Table 3 gives the values of the separation point ξ_s and the corresponding values of $-\theta(\xi_s, 0)$.

It is also of interest to note that a special procedure is needed to obtained the solution at the separation point. The reason being that the behavior of f'' vs ξ in the neighborhood of the separation point is dual. Thus by marching from the known solution of the forced

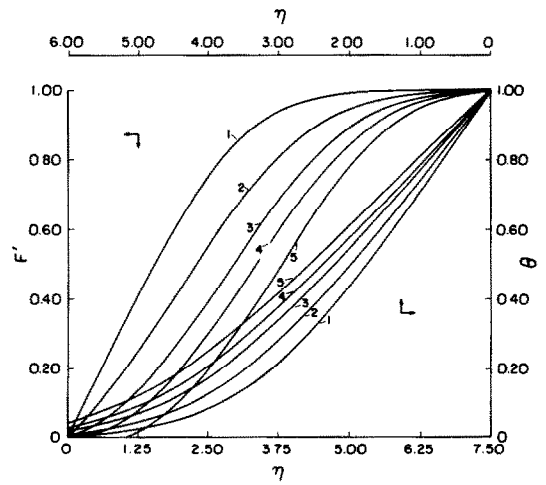

FIG. 9. Temperature and velocity profiles for opposing mixed convective flow over horizontal surfaces, for $Pr = 0.7$. Curves 1–5 designate $\xi_2 = 0.0$, 0.0566, 0.0826, 0.0896, and 0.0929, respectively.

Table 3. Results of $-\theta'(\xi_s, 0)$ at separation from rigorous solution

	Vertical plate		Horizontal plate	
Pr	$(Gr/Re^2)_s$	$-\theta'(\xi, 0)$	$(Gr/Re^{5/2})_s$	$-\theta'(\xi, 0)$
0.1	0.1437	0.0989	0.0299	0.1135
0.7	0.1865	0.1763	0.0850	0.2101
1.0	0.1928	0.1846	0.1062	0.2351
10.0	0.3132	0.3648	0.5281	0.5010

convection limit, only the upper part of the solution curve can be reached while the separation point lies in the lower part of the curve. To circumvent this difficulty, equations (18) and (19) are first solved with $f''(\xi, 0) = 0$ instead of the boundary condition, equation (20b). We then march in the direction of ξ until the boundary conditions, equation (20b), is satisfied to an accuracy of 10^{-3}.

5. CONCLUSIONS

The introduction of the mixed-convective parameters $\xi = (1 + Gr^2/Re^4)^{-1}$ and $(1 + Gr^2/Re^5)^{-1}$, respectively, in the nondimensionalization of the governing equations describing the mixed, forced and free convection flow over vertical and horizontal flat surfaces provides solutions which are uniformly valid over the entire range of mixed-flow intensities. The formulation of the resulting equations is such that the forced and free flow equations are respectively recovered from values of the mixed convection parameter $\xi = 1.0$ or 0. The solutions of the respective problems provide smooth transition of the physical variables from one convective limit to the other.

Since $\xi \sim (1 + \text{const.} \cdot x^2)^{-1}$ for flow over a vertical plate, therefore the structure of the boundary layer varies from forced convection dominated near the leading edge to natural convection dominated as the distance from the leading edge increases. Similar behavior holds for the convective flow over a horizontal plate, where $\xi \sim (1 + \text{const.} \cdot x)^{-1}$.

Comparison of the results obtained from the rigorous numerical solution and the local similarity approximation shows that the local similarity solution provides reasonable results for the wall values of $F''(\xi, 0)$ and $\theta'(\xi, 0)$, although there is considerable deviation of the velocity profiles away from the wall in the range of intense mixed convection. The present study has also determined the separation points in opposing flows and simple approximate relationships for local Nusselt numbers over the entire range of mixed convection intensities and over the range of Prandtl numbers considered. For the horizontal case it is further found that the behavior of $f''(\xi, 0)$ vs ξ in the neighborhood of the separation point is dual in that two different values of $f''(\xi, 0)$ can exist for a given ξ.

Acknowledgements—This work was supported by the Heat Transfer Program of NSF under Grant No. MEA-8121779. X.Q.L. was on sabbatical leave from the Chemical Machinery Research Institute, Lanzhou, China. We thank Professors

Richard O. Buckius and Roger A. Strehlow of the University of Illinois, Urbana-Champaign, for their arrangement to have some of the computing work done there.

REFERENCES

1. N. Ramachandran, B. F. Armaly and T. S. Chen, Mixed convection over a horizontal heated flat plate, ASME Paper 82-HT-75 (1982).
2. T. S. Chen, E. M. Sparrow and A. Mucoglu, Mixed convection in boundary layer flows on a horizontal flat plate, *Trans. Am. Soc. Mech. Engrs*, Series C, *J. Heat Transfer* **101**, 422–426 (1979).
3. E. M. Sparrow and W. J. Minkowycz, Buoyancy effects on horizontal boundary-layer flow and heat transfer, *Int. J. Heat Mass Transfer* **5**, 505–511 (1962).
4. L. C. Redekopp and A. F. Charwat, Role of buoyancy and the Boussinesq approximation in horizontal boundary layers, *J. Hydronautics* **6**, 34–39 (1972).
5. G. E. Robertson, J. H. Seinfeld and G. E. Leal, Combined forced and free convection flow past a horizontal flat plate, *A.I.Ch.E. Jl* **19**, 998–1008 (1973).
6. C. A. Hieber, Mixed convection above a heated horizontal surface, *Int. J. Heat Mass Transfer* **16**, 769–785 (1973).
7. A. Mucoglu and T. S. Chen, Mixed convection on inclined surfaces, *Trans. Am. Soc. Mech. Engrs*, Series C, *J. Heat Transfer* **101**, 422–426 (1979).
8. J. H. Merkin, The effect of buoyancy forces on the boundary-layer flow over a semi-infinite vertical flat plate in a uniform free stream, *J. Fluid Mech.* **35**, 439–450 (1969).
9. E. M. Sparrow and J. L. Gregg, Buoyancy effects in forced-convection flow and heat-transfer, *Trans. Am. Soc. Mech. Engrs*, Series E, *J. Appl. Mech.* **81**, 133–134 (1959).
10. J. R. Lloyd and E. M. Sparrow, Combined forced and free convection flow on vertical surfaces, *Int. J. Heat Mass Transfer* **13**, 434–438 (1970).
11. G. Wilks, Combined forced and free convection flow on vertical surfaces, *Int. J. Heat Mass Transfer* **16**, 1958–1964 (1973).
12. A. C. Fernandez-Pello and C. K. Law, On the mixed-convective flame structure in the stagnation point of a fuel particle, 19th Symp. (Int.) on Combustion, pp. 1037–1044 (1983).
13. A. C. Fernandez-Pello and P. J. Pagni, Mixed convective burning of a vertical fuel surface, *Proc. ASME–JSME Thermal Engineering Joint Conf.*, Vol. 4, pp. 295–301 (1983).
14. E. M. Sparrow and H. S. Yu, Local non-similarity thermal boundary-layer solutions. *Trans. Am. Soc. Mech. Engrs*, Series C, *J. Heat Transfer* **93**, 328–334 (1971).
15. T. Y. Na, Computational methods in engineering boundary value problems, in *Mathematics in Science and Engineering*, Vol. 145. Academic Press, New York (1979).
16. H. B. Keller and T. Cebeci, Accurate numerical methods for boundary-layer flows. I: Two-dimensional laminar flows, *Proc. 2nd Int. Conf. on Numerical Methods in Fluid Dynamics*. Springer, Berlin (1971).
17. H. B. Keller and T. Cebeci, Accurate numerical methods for boundary-layer flows. II: Two dimensional turbulent flows, *AIAA J.* **10**, 1193–1199 (1972).
18. A. S. Householder, *The Theory of Matrices in Numerical Analysis*. Blaisdell (1964).

APPENDIX

The method of quasi-linearization is quite straightforward in its application to non-linear ordinary and partial differential equations of parabolic type [15]. If the integral boundary condition in equation (20b) is evaluated from the current approximate solution of the recurrence equation, the resulting procedure is extremely time consuming if at all it converges. The proposed method inherits all the general features of quasi-linearization including quadratic convergence and monotone convergence, and retains the tridiagonal block structure of the matrix which can be efficiently solved using Keller's scheme [16, 17].

For convenience, the governing equations of mixed-convective flow over a horizontal flat plate are written as

$$F'''' + A(\xi)FF''' + B(\xi)F'F'' + C(\xi)\eta\theta' + D(\xi)\frac{\partial\theta}{\partial\xi} + E(\xi)F'''\frac{\partial F}{\partial\xi} + G(\xi)F'\frac{\partial F''}{\partial\xi} = 0 \quad \text{(A1)}$$

$$\theta'' + H(\xi, Pr)\theta'F + I(\xi, Pr)\theta'\frac{\partial F}{\partial\xi} + J(\xi, Pr)F'\frac{\partial\theta}{\partial\xi} = 0 \quad \text{(A2)}$$

where $A, B, \ldots, J$ correspond to the constants involving ξ and Pr in equations (18) and (19) and can be obtained by comparison. Let the net points of the finite-difference equations be given by

$$\xi_0 = 0, \quad \xi_k = \xi_{k-1} + l, \quad l = 1, 2, \ldots, N$$

$$\eta_0 = 0, \quad \eta = n_{n-1} + h, \quad h = 1, 2, \ldots, J$$

where h is a constant and l can be non-uniform as it is required to find the solution for $\{F, \theta\}$ from $0 < n < J$ at k when $\{F, \theta\}$ are known for $0 < n < J$ at $k-1$. At $\xi = \xi_k$ the method of quasi-linearization yields the following recurrence relationship for equations (A1) and (A2)

$$\begin{aligned} &F''''^{i+1} + F'''^{i+1}\left[AF^i + E\frac{\partial F^i}{\partial\xi}\right] + F''^{i+1}[BF'^i] \\ &+ F'^{i+1}\left[BF''^i + G\frac{\partial F''^i}{\partial\xi}\right] + F^{i+1}[AF''''^i] \\ &+ \theta'^{i+1}[C\eta] + \frac{\partial\theta^{i+1}}{\partial\xi}[D] \\ &+ \frac{\partial F^{i+1}}{\partial\xi}[EF''''^i] + \frac{\partial F''^{i+1}}{\partial\xi}[GF'^i] \\ &= AF''''^iF^i + EF''''^i\frac{\partial F^i}{\partial\xi} + BF''^iF'^i + GF'^i\frac{\partial F''^i}{\partial\xi} \end{aligned} \quad \text{(A3)}$$

$$\begin{aligned} &\theta''^{i+1} + \theta'^{i+1}\left[HF^i + I\frac{\partial F^i}{\partial\xi}\right] + \frac{\partial\theta^{i+1}}{\partial\xi}[JF'^i] \\ &+ F^{i+1}[H\theta'^i] + F'\left[J\frac{\partial\theta^i}{\partial\xi}\right] + \frac{\partial F^{i+1}}{\partial\xi}[I\theta'^i] \\ &= H\theta'^iF^i + I\theta'^i\frac{\partial F^i}{\partial\xi} + JF'^i\frac{\partial\theta^i}{\partial\xi}. \end{aligned} \quad \text{(A4)}$$

The next step in the computational procedure is to reduce the above equations in terms of first- and second-order partial differential equations

$$F'^{i+1} = u^{i+1} \quad \text{(A5)}$$

$$u'^{i+1} = v^{i+1} \quad \text{(A6)}$$

$$\begin{aligned} &v''^{i+1} + v'^{i+1}\left[AF^i + E\frac{\partial F^i}{\partial\xi}\right] + \frac{\partial v^{i+1}}{\partial\xi}[Gu^i] \\ &+ v^{i+1}[Bu^i] + u^{i+1}\left[Bv^i + G\frac{\partial v^i}{\partial\xi}\right] \\ &+ F^{i+1}[Av'^i] + \frac{\partial F^{i+1}}{\partial\xi}[Ev'^i] \\ &+ \theta'^{i+1}[C\eta] + \frac{\partial\theta^{i+1}}{\partial\xi}[D] = Av'^iF^i \\ &+ Ev'^i\frac{\partial F^i}{\partial\xi} + Bv^iu^i + Gu^i\frac{\partial v^i}{\partial\xi} \end{aligned} \quad \text{(A7)}$$

$$\theta'^{i+1}+\theta'^{i+1}\left[HF^i+I\frac{\partial F^i}{\partial\xi}\right]+\frac{\partial\theta^{i+1}}{\partial\xi}[Ju^i]$$
$$+F^{i+1}[H\theta'^i]+u^{i+1}\left[J\frac{\partial\theta^i}{\partial\xi}\right]+\frac{\partial F^{i+1}}{\partial\xi}[I\theta'^i]$$
$$=H\theta'^iF^i+I\theta'^i\frac{\partial F^i}{\partial\xi}+Ju^i\frac{\partial\theta^i}{\partial\xi}. \quad \text{(A8)}$$

In finite-difference form the above equations become

$$F_{n-1}^{i+1}+\frac{h}{2}u_{n-1}^{i+1}-F_n^{i+1}+\frac{h}{2}u_n^{i+1}=0 \quad \text{(A9)}$$

$$u_{n-1}^{i+1}+\frac{h}{2}v_{n-1}^{i+1}-u_n^{i+1}+\frac{h}{2}v_n^{i+1}=0 \quad \text{(A10)}$$

$$v_{n-1}^{i+1}\left\{1-\frac{h}{2}\left[AF_n^i+E\left\{\frac{2}{l}(F_n^i-F_n^{k-1})-\frac{\partial F}{\partial\xi}\Big|_n^{k-1}\right\}\right]\right\}$$
$$+v_n^{i+1}\left\{-2+h^2\left(Bu_n^i+\frac{2}{l}Gu_n^i\right)\right\}$$
$$+v_{n+1}^{i+1}\left\{1+\frac{h}{2}\left[AF_n^i+E\left\{\frac{2}{l}(F_n^i-F_n^{k-1})-\frac{\partial F}{\partial\xi}\Big|_n^{k-1}\right\}\right]\right\}$$
$$+\theta_{n-1}^{i+1}\left\{-\frac{h}{2}C\eta_n\right\}+\theta_n^{i+1}\left\{\frac{2h^2D}{l}\right\}+\theta_{n+1}^{i+1}\left\{\frac{h}{2}C\eta_n\right\}$$
$$+F_n^{i+1}\left\{\frac{h}{2}(v_{n+1}^i-v_{n-1}^i)\left(A+\frac{2E}{l}\right)\right\}$$
$$+u_n^{i+1}\left\{h^2\left(Bv_n^i+G\left[\frac{2}{l}(v_n^i-v_n^{k-1})-\frac{\partial v}{\partial\xi}\Big|_n^{k-1}\right]\right)\right\}$$
$$=h^2\left\{\left(A+\frac{2}{l}E\right)\left(\frac{v_{n+1}^i-v_{n-1}^i}{2h}\right)F_n^i+v_n^iu_n^i\left\{B+\frac{2G}{l}\right\}\right.$$
$$\left.+\frac{2D}{l}\theta_n^{k-1}+\frac{\partial\theta}{\partial\xi}\Big|_n^{k-1}\right\} \quad \text{(A11)}$$

$$\theta_{n-1}^{i+1}\left\{1-\frac{h}{2}\left[HF_n^i+I\left\{\frac{2}{l}(F_n^i-F_n^{k-1})-\frac{\partial F}{\partial\xi}\Big|_n^{k-1}\right\}\right]\right\}$$
$$+\theta_n^{i+1}\left\{-2+\frac{2h^2}{l}Ju_n^i\right\}+\theta_{n+1}^{i+1}\left\{1+\frac{h}{2}\right.$$
$$\times\left.\left[HF_n^i+I\left\{\frac{2}{l}(F_n^i-F_n^{k-1})-\frac{\partial F}{\partial\xi}\Big|_n^{k-1}\right\}\right]\right\}$$
$$+F_n^{i+1}\left\{\frac{h}{2}\{\theta_{n+1}^i-\theta_{n-1}^i\}\left(H+\frac{2I}{l}\right)\right\}$$
$$+u_n^{i+1}\left\{h^2J\left[\frac{2}{l}(\theta_n^i-\theta_n^{k-1})-\frac{\partial\theta}{\partial\xi}\Big|_n^{k-1}\right]\right\}$$
$$=h^2\left\{\left(H+\frac{2I}{l}\right)(\theta_{n+1}^i-\theta_{n-1}^i)\frac{F_n^i}{2h}+\frac{2}{l}Ju_n^i\theta_n^i\right\}. \quad \text{(A12)}$$

In deriving the last two equations the following difference formulae are used for the derivatives

$$\frac{\partial z}{\partial\eta}=\frac{z_{n+1}-z_{n-1}}{2h}$$
$$\frac{\partial^2z}{\partial\eta^2}=\frac{z_{n+1}-2z_n+z_{n-1}}{h^2}$$
$$\frac{\partial z}{\partial\xi}=\frac{2}{l}(z_k-z_{k-1})-\frac{\partial z}{\partial\xi}\Big|_{k-1}$$

where $z=F, u, v$ or θ.

Treatment of the boundary conditions, equations (20a) and (20c), are not detailed in the discussion since they present no particular difficulty. The integral boundary condition, equation (20b), can be written as

$$v'(\xi,0)=v_1'^{i+1}=-C(\xi)\int_0^\infty\theta\,d\eta+D(\xi)\int_0^\infty\frac{\partial\theta}{\partial\xi}\,d\eta. \quad \text{(A13)}$$

By using a three-point formula for the derivative and trapezoidal rule for evaluating the integrals in the above equation, we get

$$v_1^{i+1}=\tfrac{4}{3}v_2^{i+1}-\tfrac{1}{3}v_3^{i+1}+\tfrac{2}{3}h^2\left(C-\frac{2D}{l}\right)$$
$$\times\{\tfrac{1}{2}\theta_1^{i+1}+\theta_2^{i+1}+\theta_3^{i+1}+\cdots+\theta_{N-1}^{i+1}+\tfrac{1}{2}\theta_N^{i+1}\}$$
$$+\tfrac{2}{3}h^2D\left\{\frac{1}{2}\left(\frac{2}{l}\theta_1^{k-1}+\frac{\partial\theta}{\partial\xi}\Big|_1^{k-1}\right)\right.$$
$$\left.+\left(\frac{2}{l}\theta_2^{k-1}+\frac{\partial\theta}{\partial\xi}\Big|_2^{k-1}\right)+\cdots\ \frac{1}{2}\left(\frac{2}{l}\theta_N^{k-1}+\frac{\partial\theta}{\partial\xi}\Big|_N^{k-1}\right)\right\}. \quad \text{(A14)}$$

In matrix-vector form, equations (A11), (A12) and (A14) can be written as

$$\mathbf{AX}=\mathbf{Y}. \quad \text{(A15)}$$

The matrix **A** exhibits tridiagonal block structure except for one row involving the boundary condition, equation (A14). The computational problems might be considerably reduced in inverting the matrix **A** if we let **B** be the matrix of elements containing the tridiagonal block structure and treat the remaining elements arising out of the integral boundary condition as perturbations. Equation (A15) can then be rewritten as

$$(\mathbf{B}+\mathbf{P})\mathbf{X}=\mathbf{Y} \quad \text{(A16)}$$

where **P** is the perturbed matrix. In what follows we use the Woodbury formula [18] which avoids the explicit inversion of the matrix **A** [18]. A perturbation matrix **P** can always be expressed as a product $\mathbf{USV}^T$. In our case, the matrix **P** consisting of only one non-zero row $\mathbf{V}_1$, in the r_1 position, is given by the product $\mathbf{UV}^T$ where

$$\mathbf{U}=[e(r_1)]$$

and

$$\mathbf{V}=[\mathbf{V}_1^T]$$

and **S** which is an identity matrix becomes a scalar 1 in the present problem. For the Woodbury formula let **Q** be the solution to

$$\mathbf{BQ}=\mathbf{U} \quad \text{(A17)}$$

and let **R** be the solution to

$$(1+\mathbf{V}^T\mathbf{Q})\mathbf{R}=\mathbf{V}^T,$$

Then the solution to $(\mathbf{B}+\mathbf{P})\mathbf{X}=\mathbf{Y}$, where $\mathbf{P}=\mathbf{USV}^T$, is

$$\mathbf{X}=(\mathbf{I}-\mathbf{QR})\mathbf{X}_0=\mathbf{X}_0-\mathbf{Q}(\mathbf{RX}_0) \quad \text{(A18)}$$

where $\mathbf{X}_0$ is the solution to

$$\mathbf{BX}_0=\mathbf{Y}. \quad \text{(A19)}$$

The Woodbury formula as shown in Householder [18] simply reduces the problem of solving equation (A15) to the problem of solving equations (A17)–(A19) involving the matrix **B** of tridiagonal block structure which can be solved most efficiently using Keller's scheme [16, 17]. Unlike the reported problems of convergence encountered in obtaining a numerical solution of a similar problem in ref. [1], the present procedure is quite fast in its convergence rate. It almost always converged to an accuracy of 1 in 10^{14} in just eight iterations.

FORMULATION DE LA CONVECTION MIXTE SUR DES SURFACES HORIZONTALES ET VERTICALES

Résumé—L'écoulement à couche limite sur une plaque semi-infinie verticale ou horizontale, chauffée à température constante dans un écoulement libre uniforme, est étudié lorsque la force de pesanteur favorise ou s'oppose au développement de la couche limite. Différents paramètres de convection mixte sont introduits dans la formulation des problèmes concernant des surfaces horizontales et verticales de façon qu'une transition douce soit possible entre les deux ; en particulier les équations pour les cas de convection pure forcée et naturelle sont retrouvées en faisant respectivement les nombres de Grashof et de Reynolds nuls. Un schéma numérique est développé pour incorporer la condition intégrale limite qui apparait dans les équations de l'écoulement sur une plaque plane horizontale, ce qui rend possible la convergence numérique. Des solutions localement semblables et non semblables sont aussi obtenues. Elles montrent un écart considérable des profils de vitesse par rapport à la solution rigoureuse par différence finie dans la région de la convection mixte intense, bien qu'un bon accord existe pour les valeurs à la paroi, comme le représentent les facteurs de frottement et les nombres de Nusselt, lesquels sont d'intérêt primordial. Des expressions explicites simples entre les nombres de Nusselt locaux sont données pour le domaine entier de convection mixte quand le nombre de Prandtl varie entre 0,1 et 10. Les points de séparation sont aussi obtenus pour les écoulements en opposition.

EINE BESCHREIBUNG DER ÜBERLAGERTEN FREIEN UND ERZWUNGENEN KONVEKTION AN HORIZONTALEN UND VERTIKALEN OBERFLÄCHEN

Zusammenfassung—Es wird die Grenzschichtströmung an halbunendlichen senkrechten und waagerechten ebenen Platten, die durch eine gleichförmige freie Strömung auf konstanten Temperaturen gehalten werden, für die Fälle untersucht, in denen die Schwerkräfte entweder die Ausbildung der Grenzschicht begünstigen oder behindern. Es wurden verschiedene Parameter für überlagerte Konvektion bei der Formulierung der betreffenden Probleme, die horizontale und vertikale Oberflächen einschließen, so eingeführt, daß ein stetiger Übergang von der einen zur anderen Konvektionsform möglich ist; insbesondere ergeben sich die gültigen Gleichungen für rein erzwungene Konvektion bzw. reine freie Konvektion, wenn die Grashof-Zahl bzw. die Reynolds-Zahl null gesetzt wird. Es wird ein wirksames numerisches Verfahren entwickelt, um die Randbedingung in integraler Form, die in den Bestimmungsgleichungen für die Strömung an einer horizontalen ebenen Platte auftritt, zu berücksichtigen, wodurch numerische Konvergenz erreicht wird. Örtlich ähnliche und nichtähnliche Lösungen werden in gleicher Weise erhalten. Diese zeigen beträchtliche Abweichungen der Geschwindigkeitsprofile von der strengen Lösung mittels finiter Differenzen im Gebiet der stark überlagerten Konvektion, obwohl gute Übereinstimmung für die Werte an der Wand besteht, die durch die vorrangig interessierenden Widerstandsbeiwerte und Nusselt-Zahlen gegeben sind. Es werden einfache explizite Ausdrücke bestimmt, welche die Nusselt-Zahlen im ganzen Bereich der überlagerten Konvektion wiedergeben, wobei die *Pr*-Zahlen von 0,1 bis 10 variieren. Die Ablösungspunkte mit Rückströmung werden gleichfalls erhalten.

ФОРМУЛИРОВКА УРАВНЕНИЙ СОВМЕСТНОЙ ВЫНУЖДЕННОЙ И СВОБОДНОЙ КОНВЕКЦИИ У ГОРИЗОНТАЛЬНЫХ И ВЕРТИКАЛЬНЫХ ПОВЕРХНОСТЕЙ

Аннотация—Исследуется течение в пограничном слое на полубесконечных вертикальных и горизонтальных пластинах, нагреваемых до постоянной температуры в однородном свободном потоке, когда силы плавучести способствуют или противодействуют развитию пограничного слоя. Для формулировки соответствующих задач, включающих горизонтальные и вертикальные поверхности, использованы различные параметры смешанной конвекции, обеспечивающие плавный переход от одного конвективного предела к другому; в частности, основные уравнения для чисто вынужденной и чисто свободной конвекции, соответственно, выводятся при нулевых значениях чисел Грасгофа и Рейнольдса. Предложена эффективная численная схема, в которой используется интегральное граничное условие совместно с основными уравнениями для потока на горизонтальной плоской пластине, тем самым позволяя получить численную сходимость. Получены также автомодельные и неавтомодельные решения, из которых видно, что профили скорости значительно отклоняются от профилей, рассчитанных точным конечно-разностным методом для области интенсивной смешанной конвекции. В то же время хорошее совпадение получено для таких величин на стенке, как коэффициент трения и число Нуссельта, представляющих основной интерес. Выведены простые соотношения в явном виде для локальных чисел Нуссельта в широком диапазоне интенсивностей смешанной конвекции при изменении числа Прандтля от 0,1 до 10. Определены также точки отрыва в противоположно направленных потоках.